



Observation of Z production in proton-lead collisions at LHCb

The LHCb collaboration[†]

Abstract

The first observation of Z boson production in proton-lead collisions at a centre-of-mass energy per proton-nucleon pair of $\sqrt{s_{NN}} = 5$ TeV is presented. The data sample corresponds to an integrated luminosity of 1.6 nb^{-1} collected with the LHCb detector. The Z candidates are reconstructed from pairs of oppositely charged muons with pseudorapidities between 2.0 and 4.5 and transverse momenta above $20 \text{ GeV}/c$. The invariant dimuon mass is restricted to the range $60 - 120 \text{ GeV}/c^2$. The Z production cross-section is measured to be

$$\sigma_{Z \rightarrow \mu^+ \mu^-}(\text{fwd}) = 13.5_{-4.0}^{+5.4}(\text{stat.}) \pm 1.2(\text{syst.}) \text{ nb}$$

in the direction of the proton beam and

$$\sigma_{Z \rightarrow \mu^+ \mu^-}(\text{bwd}) = 10.7_{-5.1}^{+8.4}(\text{stat.}) \pm 1.0(\text{syst.}) \text{ nb}$$

in the direction of the lead beam, where the first uncertainty is statistical and the second systematic.

Published in JHEP 09 (2014) 030

© CERN on behalf of the LHCb collaboration, license CC-BY-3.0.

[†]Authors are listed on the following pages.

LHCb collaboration

R. Aaij⁴¹, B. Adeva³⁷, M. Adinolfi⁴⁶, A. Affolder⁵², Z. Ajaltouni⁵, S. Akar⁶, J. Albrecht⁹, F. Alessio³⁸, M. Alexander⁵¹, S. Ali⁴¹, G. Alkhazov³⁰, P. Alvarez Cartelle³⁷, A.A. Alves Jr^{25,38}, S. Amato², S. Amerio²², Y. Amhis⁷, L. An³, L. Anderlini^{17,g}, J. Anderson⁴⁰, R. Andreassen⁵⁷, M. Andreotti^{16,f}, J.E. Andrews⁵⁸, R.B. Appleby⁵⁴, O. Aquines Gutierrez¹⁰, F. Archilli³⁸, A. Artamonov³⁵, M. Artuso⁵⁹, E. Aslanides⁶, G. Auriemma^{25,n}, M. Baalouch⁵, S. Bachmann¹¹, J.J. Back⁴⁸, A. Badalov³⁶, V. Balagura³¹, W. Baldini¹⁶, R.J. Barlow⁵⁴, C. Barschel³⁸, S. Barsuk⁷, W. Barter⁴⁷, V. Batozskaya²⁸, V. Battista³⁹, A. Bay³⁹, L. Beaucourt⁴, J. Beddow⁵¹, F. Bedeschi²³, I. Bediaga¹, S. Belogurov³¹, K. Belous³⁵, I. Belyaev³¹, E. Ben-Haim⁸, G. Bencivenni¹⁸, S. Benson³⁸, J. Benton⁴⁶, A. Berezhnoy³², R. Bernet⁴⁰, M.-O. Bettler⁴⁷, M. van Beuzekom⁴¹, A. Bien¹¹, S. Bifani⁴⁵, T. Bird⁵⁴, A. Bizzeti^{17,i}, P.M. Bjørnstad⁵⁴, T. Blake⁴⁸, F. Blanc³⁹, J. Blouw¹⁰, S. Blusk⁵⁹, V. Bocci²⁵, A. Bondar³⁴, N. Bondar^{30,38}, W. Bonivento^{15,38}, S. Borghi⁵⁴, A. Borgia⁵⁹, M. Borsato⁷, T.J.V. Bowcock⁵², E. Bowen⁴⁰, C. Bozzi¹⁶, T. Brambach⁹, J. van den Brand⁴², J. Bressieux³⁹, D. Brett⁵⁴, M. Britsch¹⁰, T. Britton⁵⁹, J. Brodzicka⁵⁴, N.H. Brook⁴⁶, H. Brown⁵², A. Bursche⁴⁰, G. Busetto^{22,r}, J. Buytaert³⁸, S. Cadeddu¹⁵, R. Calabrese^{16,f}, M. Calvi^{20,k}, M. Calvo Gomez^{36,p}, A. Camboni³⁶, P. Campana^{18,38}, D. Campora Perez³⁸, A. Carbone^{14,d}, G. Carboni^{24,l}, R. Cardinale^{19,38,j}, A. Cardini¹⁵, H. Carranza-Mejia⁵⁰, L. Carson⁵⁰, K. Carvalho Akiba², G. Casse⁵², L. Cassina²⁰, L. Castillo Garcia³⁸, M. Cattaneo³⁸, Ch. Cauet⁹, R. Cenci⁵⁸, M. Charles⁸, Ph. Charpentier³⁸, S. Chen⁵⁴, S.-F. Cheung⁵⁵, N. Chiapolini⁴⁰, M. Chrzaszcz^{40,26}, K. Ciba³⁸, X. Cid Vidal³⁸, G. Ciezarek⁵³, P.E.L. Clarke⁵⁰, M. Clemencic³⁸, H.V. Cliff⁴⁷, J. Closier³⁸, V. Coco³⁸, J. Cogan⁶, E. Cogneras⁵, P. Collins³⁸, A. Comerma-Montells¹¹, A. Contu¹⁵, A. Cook⁴⁶, M. Coombes⁴⁶, S. Coquereau⁸, G. Corti³⁸, M. Corvo^{16,f}, I. Counts⁵⁶, B. Couturier³⁸, G.A. Cowan⁵⁰, D.C. Craik⁴⁸, M. Cruz Torres⁶⁰, S. Cunliffe⁵³, R. Currie⁵⁰, C. D'Ambrosio³⁸, J. Dalseno⁴⁶, P. David⁸, P.N.Y. David⁴¹, A. Davis⁵⁷, K. De Bruyn⁴¹, S. De Capua⁵⁴, M. De Cian¹¹, J.M. De Miranda¹, L. De Paula², W. De Silva⁵⁷, P. De Simone¹⁸, D. Decamp⁴, M. Deckenhoff⁹, L. Del Buono⁸, N. Déleage⁴, D. Derkach⁵⁵, O. Deschamps⁵, F. Dettori³⁸, A. Di Canto³⁸, H. Dijkstra³⁸, S. Donleavy⁵², F. Dordei¹¹, M. Dorigo³⁹, A. Dosil Suárez³⁷, D. Dossett⁴⁸, A. Dovbnya⁴³, K. Dreimanic⁵², G. Dujany⁵⁴, F. Dupertuis³⁹, P. Durante³⁸, R. Dzhelyadin³⁵, A. Dziurda²⁶, A. Dzyuba³⁰, S. Easo^{49,38}, U. Egede⁵³, V. Egorychev³¹, S. Eidelman³⁴, S. Eisenhardt⁵⁰, U. Eitschberger⁹, R. Ekelhof⁹, L. Eklund^{51,38}, I. El Rifai⁵, Ch. Elsasser⁴⁰, S. Ely⁵⁹, S. Esen¹¹, H.-M. Evans⁴⁷, T. Evans⁵⁵, A. Falabella¹⁴, C. Färber¹¹, C. Farinelli⁴¹, N. Farley⁴⁵, S. Farry⁵², R.F. Fay⁵², D. Ferguson⁵⁰, V. Fernandez Albor³⁷, F. Ferreira Rodrigues¹, M. Ferro-Luzzi³⁸, S. Filippov³³, M. Fiore^{16,f}, M. Fiorini^{16,f}, M. Firlej²⁷, C. Fitzpatrick³⁸, T. Fiutowski²⁷, M. Fontana¹⁰, F. Fontanelli^{19,j}, R. Forty³⁸, O. Francisco², M. Frank³⁸, C. Frei³⁸, M. Frosini^{17,38,g}, J. Fu^{21,38}, E. Furfaro^{24,l}, A. Gallas Torreira³⁷, D. Galli^{14,d}, S. Gallorini²², S. Gambetta^{19,j}, M. Gandelman², P. Gandini⁵⁹, Y. Gao³, J. García Pardiñas³⁷, J. Garofoli⁵⁹, J. Garra Tico⁴⁷, L. Garrido³⁶, C. Gaspar³⁸, R. Gauld⁵⁵, L. Gavardi⁹, G. Gavrillov³⁰, E. Gersabeck¹¹, M. Gersabeck⁵⁴, T. Gershon⁴⁸, Ph. Ghez⁴, A. Gianelle²², S. Giani³⁹, V. Gibson⁴⁷, L. Giubega²⁹, V.V. Gligorov³⁸, C. Göbel⁶⁰, D. Golubkov³¹, A. Golutvin^{53,31,38}, A. Gomes^{1,a}, H. Gordon³⁸, C. Gotti²⁰, M. Grabalosa Gándara⁵, R. Graciani Diaz³⁶, L.A. Granado Cardoso³⁸, E. Graugés³⁶, G. Graziani¹⁷, A. Grecu²⁹, E. Greening⁵⁵, S. Gregson⁴⁷, P. Griffith⁴⁵, L. Grillo¹¹, O. Grünberg⁶², B. Gui⁵⁹, E. Gushchin³³, Yu. Guz^{35,38}, T. Gys³⁸, C. Hadjivasiliou⁵⁹, G. Haefeli³⁹, C. Haen³⁸, S.C. Haines⁴⁷, S. Hall⁵³, B. Hamilton⁵⁸, T. Hampson⁴⁶, X. Han¹¹, S. Hansmann-Menzemer¹¹, N. Harnew⁵⁵, S.T. Harnew⁴⁶, J. Harrison⁵⁴,

J. He³⁸, T. Head³⁸, V. Heijne⁴¹, K. Hennessy⁵², P. Henrard⁵, L. Henry⁸,
 J.A. Hernando Morata³⁷, E. van Herwijnen³⁸, M. Heß⁶², A. Hicheur¹, D. Hill⁵⁵, M. Hoballah⁵,
 C. Hombach⁵⁴, W. Hulsbergen⁴¹, P. Hunt⁵⁵, N. Hussain⁵⁵, D. Hutchcroft⁵², D. Hynds⁵¹,
 M. Idzik²⁷, P. Ilten⁵⁶, R. Jacobsson³⁸, A. Jaeger¹¹, J. Jalocha⁵⁵, E. Jans⁴¹, P. Jatón³⁹,
 A. Jawahery⁵⁸, F. Jing³, M. John⁵⁵, D. Johnson⁵⁵, C.R. Jones⁴⁷, C. Joram³⁸, B. Jost³⁸,
 N. Jurik⁵⁹, M. Kabbalo⁹, S. Kandybei⁴³, W. Kanso⁶, M. Karacson³⁸, T.M. Karbach³⁸,
 S. Karodia⁵¹, M. Kelsey⁵⁹, I.R. Kenyon⁴⁵, T. Ketel⁴², B. Khanji²⁰, C. Khurewathanakul³⁹,
 S. Klaver⁵⁴, K. Klimaszewski²⁸, O. Kochebina⁷, M. Kolpin¹¹, I. Komarov³⁹, R.F. Koopman⁴²,
 P. Koppenburg^{41,38}, M. Korolev³², A. Kozlinskiy⁴¹, L. Kravchuk³³, K. Kreplin¹¹, M. Kreps⁴⁸,
 G. Krocker¹¹, P. Krokovny³⁴, F. Kruse⁹, W. Kucewicz^{26,o}, M. Kucharczyk^{20,26,38,k},
 V. Kudryavtsev³⁴, K. Kurek²⁸, T. Kvaratskheliya³¹, V.N. La Thi³⁹, D. Lacarrere³⁸,
 G. Lafferty⁵⁴, A. Lai¹⁵, D. Lambert⁵⁰, R.W. Lambert⁴², E. Lanciotti³⁸, G. Lanfranchi¹⁸,
 C. Langenbruch³⁸, B. Langhans³⁸, T. Latham⁴⁸, C. Lazzeroni⁴⁵, R. Le Gac⁶, J. van Leerdam⁴¹,
 J.-P. Lees⁴, R. Lefèvre⁵, A. Leflat³², J. Lefrançois⁷, S. Leo²³, O. Leroy⁶, T. Lesiak²⁶,
 B. Leverington¹¹, Y. Li³, M. Liles⁵², R. Lindner³⁸, C. Linn³⁸, F. Lionetto⁴⁰, B. Liu¹⁵, G. Liu³⁸,
 S. Lohn³⁸, I. Longstaff⁵¹, J.H. Lopes², N. Lopez-March³⁹, P. Lowdon⁴⁰, H. Lu³, D. Lucchesi^{22,r},
 H. Luo⁵⁰, A. Lupato²², E. Luppi^{16,f}, O. Lupton⁵⁵, F. Machefert⁷, I.V. Machikhiliyan³¹,
 F. Maciuc²⁹, O. Maev³⁰, S. Malde⁵⁵, G. Manca^{15,e}, G. Mancinelli⁶, J. Maratas⁵, J.F. Marchand⁴,
 U. Marconi¹⁴, C. Marin Benito³⁶, P. Marino^{23,t}, R. Märki³⁹, J. Marks¹¹, G. Martellotti²⁵,
 A. Martens⁸, A. Martín Sánchez⁷, M. Martinelli⁴¹, D. Martinez Santos⁴², F. Martinez Vidal⁶⁴,
 D. Martins Tostes², A. Massafferri¹, R. Matev³⁸, Z. Mathe³⁸, C. Matteuzzi²⁰, A. Mazurov^{16,f},
 M. McCann⁵³, J. McCarthy⁴⁵, A. McNab⁵⁴, R. McNulty¹², B. McSkelly⁵², B. Meadows⁵⁷,
 F. Meier⁹, M. Meissner¹¹, M. Merk⁴¹, D.A. Milanes⁸, M.-N. Minard⁴, N. Moggi¹⁴,
 J. Molina Rodriguez⁶⁰, S. Monteil⁵, M. Morandin²², P. Morawski²⁷, A. Mordà⁶, M.J. Morello^{23,t},
 J. Moron²⁷, A.-B. Morris⁵⁰, R. Mountain⁵⁹, F. Muheim⁵⁰, K. Müller⁴⁰, R. Muresan²⁹,
 M. Mussini¹⁴, B. Muster³⁹, P. Naik⁴⁶, T. Nakada³⁹, R. Nandakumar⁴⁹, I. Nasteva²,
 M. Needham⁵⁰, N. Neri²¹, S. Neubert³⁸, N. Neufeld³⁸, M. Neuner¹¹, A.D. Nguyen³⁹,
 T.D. Nguyen³⁹, C. Nguyen-Mau^{39,q}, M. Nicol⁷, V. Niess⁵, R. Niet⁹, N. Nikitin³², T. Nikodem¹¹,
 A. Novoselov³⁵, D.P. O'Hanlon⁴⁸, A. Oblakowska-Mucha²⁷, V. Obraztsov³⁵, S. Oggero⁴¹,
 S. Ogilvy⁵¹, O. Okhrimenko⁴⁴, R. Oldeman^{15,e}, G. Onderwater⁶⁵, M. Orlandea²⁹,
 J.M. Otalora Goicochea², P. Owen⁵³, A. Oyanguren⁶⁴, B.K. Pal⁵⁹, A. Palano^{13,c}, F. Palombo^{21,u},
 M. Palutan¹⁸, J. Panman³⁸, A. Papanestis^{49,38}, M. Pappagallo⁵¹, C. Parkes⁵⁴,
 C.J. Parkinson^{9,45}, G. Passaleva¹⁷, G.D. Patel⁵², M. Patel⁵³, C. Patrignani^{19,j},
 A. Pazos Alvarez³⁷, A. Pearce⁵⁴, A. Pellegrino⁴¹, M. Pepe Altarelli³⁸, S. Perazzini^{14,d},
 E. Perez Trigo³⁷, P. Perret⁵, M. Perrin-Terrin⁶, L. Pescatore⁴⁵, E. Pesen⁶⁶, K. Petridis⁵³,
 A. Petrolini^{19,j}, E. Picatoste Olloqui³⁶, B. Pietrzyk⁴, T. Pilar⁴⁸, D. Pinci²⁵, A. Pistone¹⁹,
 S. Playfer⁵⁰, M. Plo Casasus³⁷, F. Polci⁸, A. Poluektov^{48,34}, E. Polcarpo², A. Popov³⁵,
 D. Popov¹⁰, B. Popovici²⁹, C. Potterat², E. Price⁴⁶, J. Prisciandaro³⁹, A. Pritchard⁵²,
 C. Prouve⁴⁶, V. Pugatch⁴⁴, A. Puig Navarro³⁹, G. Punzi^{23,s}, W. Qian⁴, B. Rachwal²⁶,
 J.H. Rademacker⁴⁶, B. Rakotomiaramananana³⁹, M. Rama¹⁸, M.S. Rangel², I. Raniuk⁴³,
 N. Rauschmayr³⁸, G. Raven⁴², S. Reichert⁵⁴, M.M. Reid⁴⁸, A.C. dos Reis¹, S. Ricciardi⁴⁹,
 S. Richards⁴⁶, M. Rihl³⁸, K. Rinnert⁵², V. Rives Molina³⁶, D.A. Roa Romero⁵, P. Robbe⁷,
 A.B. Rodrigues¹, E. Rodrigues⁵⁴, P. Rodriguez Perez⁵⁴, S. Roiser³⁸, V. Romanovsky³⁵,
 A. Romero Vidal³⁷, M. Rotondo²², J. Rouvinet³⁹, T. Ruf³⁸, F. Ruffini²³, H. Ruiz³⁶,
 P. Ruiz Valls⁶⁴, G. Sabatino^{25,l}, J.J. Saborido Silva³⁷, N. Sagidova³⁰, P. Sail⁵¹, B. Saitta^{15,e},
 V. Salustino Guimaraes², C. Sanchez Mayordomo⁶⁴, B. Sanmartin Sedes³⁷, R. Santacesaria²⁵,

C. Santamarina Rios³⁷, E. Santovetti^{24,l}, M. Sapunov⁶, A. Sarti^{18,m}, C. Satriano^{25,n}, A. Satta²⁴, D.M. Saunders⁴⁶, M. Savrie^{16,f}, D. Savrina^{31,32}, M. Schiller⁴², H. Schindler³⁸, M. Schlupp⁹, M. Schmelling¹⁰, B. Schmidt³⁸, O. Schneider³⁹, A. Schopper³⁸, M.-H. Schune⁷, R. Schwemmer³⁸, B. Sciascia¹⁸, A. Sciubba²⁵, M. Seco³⁷, A. Semennikov³¹, I. Sepp⁵³, N. Serra⁴⁰, J. Serrano⁶, L. Sestini²², P. Seyfert¹¹, M. Shapkin³⁵, I. Shapoval^{16,43,f}, Y. Shcheglov³⁰, T. Shears⁵², L. Shekhtman³⁴, V. Shevchenko⁶³, A. Shires⁹, R. Silva Coutinho⁴⁸, G. Simi²², M. Sirendi⁴⁷, N. Skidmore⁴⁶, T. Skwarnicki⁵⁹, N.A. Smith⁵², E. Smith^{55,49}, E. Smith⁵³, J. Smith⁴⁷, M. Smith⁵⁴, H. Snoek⁴¹, M.D. Sokoloff⁵⁷, F.J.P. Soler⁵¹, F. Soomro³⁹, D. Souza⁴⁶, B. Souza De Paula², B. Spaan⁹, A. Sparkes⁵⁰, P. Spradlin⁵¹, F. Stagni³⁸, M. Stahl¹¹, S. Stahl¹¹, O. Steinkamp⁴⁰, O. Stenyakin³⁵, S. Stevenson⁵⁵, S. Stoica²⁹, S. Stone⁵⁹, B. Storaci⁴⁰, S. Stracka^{23,38}, M. Straticiu²⁹, U. Straumann⁴⁰, R. Stroili²², V.K. Subbiah³⁸, L. Sun⁵⁷, W. Sutcliffe⁵³, K. Swientek²⁷, S. Swientek⁹, V. Syropoulos⁴², M. Szczekowski²⁸, P. Szczypka^{39,38}, D. Szilard², T. Szumlak²⁷, S. T'Jampens⁴, M. Teklishyn⁷, G. Tellarini^{16,f}, F. Teubert³⁸, C. Thomas⁵⁵, E. Thomas³⁸, J. van Tilburg⁴¹, V. Tisserand⁴, M. Tobin³⁹, S. Tolk⁴², L. Tomassetti^{16,f}, D. Tonelli³⁸, S. Topp-Joergensen⁵⁵, N. Torr⁵⁵, E. Tournefier⁴, S. Tourneur³⁹, M.T. Tran³⁹, M. Tresch⁴⁰, A. Tsaregorodtsev⁶, P. Tsopelas⁴¹, N. Tuning⁴¹, M. Ubeda Garcia³⁸, A. Ukleja²⁸, A. Ustyuzhanin⁶³, U. Uwer¹¹, V. Vagnoni¹⁴, G. Valenti¹⁴, A. Vallier⁷, R. Vazquez Gomez¹⁸, P. Vazquez Regueiro³⁷, C. Vázquez Sierra³⁷, S. Vecchi¹⁶, J.J. Velthuis⁴⁶, M. Veltri^{17,h}, G. Veneziano³⁹, M. Vesterinen¹¹, B. Viaud⁷, D. Vieira², M. Vieites Diaz³⁷, X. Vilasis-Cardona^{36,p}, A. Vollhardt⁴⁰, D. Volyanskyy¹⁰, D. Voong⁴⁶, A. Vorobyev³⁰, V. Vorobyev³⁴, C. Voß⁶², H. Voss¹⁰, J.A. de Vries⁴¹, R. Waldi⁶², C. Wallace⁴⁸, R. Wallace¹², J. Walsh²³, S. Wandernoth¹¹, J. Wang⁵⁹, D.R. Ward⁴⁷, N.K. Watson⁴⁵, D. Websdale⁵³, M. Whitehead⁴⁸, J. Wicht³⁸, D. Wiedner¹¹, G. Wilkinson⁵⁵, M.P. Williams⁴⁵, M. Williams⁵⁶, F.F. Wilson⁴⁹, J. Wimberley⁵⁸, J. Wishahi⁹, W. Wislicki²⁸, M. Witek²⁶, G. Wormser⁷, S.A. Wotton⁴⁷, S. Wright⁴⁷, S. Wu³, K. Wyllie³⁸, Y. Xie⁶¹, Z. Xing⁵⁹, Z. Xu³⁹, Z. Yang³, X. Yuan³, O. Yushchenko³⁵, M. Zangoli¹⁴, M. Zavertyaev^{10,b}, L. Zhang⁵⁹, W.C. Zhang¹², Y. Zhang³, A. Zhelezov¹¹, A. Zhokhov³¹, L. Zhong³, A. Zvyagin³⁸.

¹ Centro Brasileiro de Pesquisas Físicas (CBPF), Rio de Janeiro, Brazil

² Universidade Federal do Rio de Janeiro (UFRJ), Rio de Janeiro, Brazil

³ Center for High Energy Physics, Tsinghua University, Beijing, China

⁴ LAPP, Université de Savoie, CNRS/IN2P3, Annecy-Le-Vieux, France

⁵ Clermont Université, Université Blaise Pascal, CNRS/IN2P3, LPC, Clermont-Ferrand, France

⁶ CPPM, Aix-Marseille Université, CNRS/IN2P3, Marseille, France

⁷ LAL, Université Paris-Sud, CNRS/IN2P3, Orsay, France

⁸ LPNHE, Université Pierre et Marie Curie, Université Paris Diderot, CNRS/IN2P3, Paris, France

⁹ Fakultät Physik, Technische Universität Dortmund, Dortmund, Germany

¹⁰ Max-Planck-Institut für Kernphysik (MPIK), Heidelberg, Germany

¹¹ Physikalisches Institut, Ruprecht-Karls-Universität Heidelberg, Heidelberg, Germany

¹² School of Physics, University College Dublin, Dublin, Ireland

¹³ Sezione INFN di Bari, Bari, Italy

¹⁴ Sezione INFN di Bologna, Bologna, Italy

¹⁵ Sezione INFN di Cagliari, Cagliari, Italy

¹⁶ Sezione INFN di Ferrara, Ferrara, Italy

¹⁷ Sezione INFN di Firenze, Firenze, Italy

¹⁸ Laboratori Nazionali dell'INFN di Frascati, Frascati, Italy

¹⁹ Sezione INFN di Genova, Genova, Italy

²⁰ Sezione INFN di Milano Bicocca, Milano, Italy

²¹ Sezione INFN di Milano, Milano, Italy

- ²² *Sezione INFN di Padova, Padova, Italy*
- ²³ *Sezione INFN di Pisa, Pisa, Italy*
- ²⁴ *Sezione INFN di Roma Tor Vergata, Roma, Italy*
- ²⁵ *Sezione INFN di Roma La Sapienza, Roma, Italy*
- ²⁶ *Henryk Niewodniczanski Institute of Nuclear Physics Polish Academy of Sciences, Kraków, Poland*
- ²⁷ *AGH - University of Science and Technology, Faculty of Physics and Applied Computer Science, Kraków, Poland*
- ²⁸ *National Center for Nuclear Research (NCBJ), Warsaw, Poland*
- ²⁹ *Horia Hulubei National Institute of Physics and Nuclear Engineering, Bucharest-Magurele, Romania*
- ³⁰ *Petersburg Nuclear Physics Institute (PNPI), Gatchina, Russia*
- ³¹ *Institute of Theoretical and Experimental Physics (ITEP), Moscow, Russia*
- ³² *Institute of Nuclear Physics, Moscow State University (SINP MSU), Moscow, Russia*
- ³³ *Institute for Nuclear Research of the Russian Academy of Sciences (INR RAN), Moscow, Russia*
- ³⁴ *Budker Institute of Nuclear Physics (SB RAS) and Novosibirsk State University, Novosibirsk, Russia*
- ³⁵ *Institute for High Energy Physics (IHEP), Protvino, Russia*
- ³⁶ *Universitat de Barcelona, Barcelona, Spain*
- ³⁷ *Universidad de Santiago de Compostela, Santiago de Compostela, Spain*
- ³⁸ *European Organization for Nuclear Research (CERN), Geneva, Switzerland*
- ³⁹ *Ecole Polytechnique Fédérale de Lausanne (EPFL), Lausanne, Switzerland*
- ⁴⁰ *Physik-Institut, Universität Zürich, Zürich, Switzerland*
- ⁴¹ *Nikhef National Institute for Subatomic Physics, Amsterdam, The Netherlands*
- ⁴² *Nikhef National Institute for Subatomic Physics and VU University Amsterdam, Amsterdam, The Netherlands*
- ⁴³ *NSC Kharkiv Institute of Physics and Technology (NSC KIPT), Kharkiv, Ukraine*
- ⁴⁴ *Institute for Nuclear Research of the National Academy of Sciences (KINR), Kyiv, Ukraine*
- ⁴⁵ *University of Birmingham, Birmingham, United Kingdom*
- ⁴⁶ *H.H. Wills Physics Laboratory, University of Bristol, Bristol, United Kingdom*
- ⁴⁷ *Cavendish Laboratory, University of Cambridge, Cambridge, United Kingdom*
- ⁴⁸ *Department of Physics, University of Warwick, Coventry, United Kingdom*
- ⁴⁹ *STFC Rutherford Appleton Laboratory, Didcot, United Kingdom*
- ⁵⁰ *School of Physics and Astronomy, University of Edinburgh, Edinburgh, United Kingdom*
- ⁵¹ *School of Physics and Astronomy, University of Glasgow, Glasgow, United Kingdom*
- ⁵² *Oliver Lodge Laboratory, University of Liverpool, Liverpool, United Kingdom*
- ⁵³ *Imperial College London, London, United Kingdom*
- ⁵⁴ *School of Physics and Astronomy, University of Manchester, Manchester, United Kingdom*
- ⁵⁵ *Department of Physics, University of Oxford, Oxford, United Kingdom*
- ⁵⁶ *Massachusetts Institute of Technology, Cambridge, MA, United States*
- ⁵⁷ *University of Cincinnati, Cincinnati, OH, United States*
- ⁵⁸ *University of Maryland, College Park, MD, United States*
- ⁵⁹ *Syracuse University, Syracuse, NY, United States*
- ⁶⁰ *Pontifícia Universidade Católica do Rio de Janeiro (PUC-Rio), Rio de Janeiro, Brazil, associated to ²*
- ⁶¹ *Institute of Particle Physics, Central China Normal University, Wuhan, Hubei, China, associated to ³*
- ⁶² *Institut für Physik, Universität Rostock, Rostock, Germany, associated to ¹¹*
- ⁶³ *National Research Centre Kurchatov Institute, Moscow, Russia, associated to ³¹*
- ⁶⁴ *Instituto de Fisica Corpuscular (IFIC), Universitat de Valencia-CSIC, Valencia, Spain, associated to ³⁶*
- ⁶⁵ *KVI - University of Groningen, Groningen, The Netherlands, associated to ⁴¹*
- ⁶⁶ *Celal Bayar University, Manisa, Turkey, associated to ³⁸*

^a *Universidade Federal do Triângulo Mineiro (UFTM), Uberaba-MG, Brazil*

^b *P.N. Lebedev Physical Institute, Russian Academy of Science (LPI RAS), Moscow, Russia*

^c *Università di Bari, Bari, Italy*

^d *Università di Bologna, Bologna, Italy*

- ^e *Università di Cagliari, Cagliari, Italy*
- ^f *Università di Ferrara, Ferrara, Italy*
- ^g *Università di Firenze, Firenze, Italy*
- ^h *Università di Urbino, Urbino, Italy*
- ⁱ *Università di Modena e Reggio Emilia, Modena, Italy*
- ^j *Università di Genova, Genova, Italy*
- ^k *Università di Milano Bicocca, Milano, Italy*
- ^l *Università di Roma Tor Vergata, Roma, Italy*
- ^m *Università di Roma La Sapienza, Roma, Italy*
- ⁿ *Università della Basilicata, Potenza, Italy*
- ^o *AGH - University of Science and Technology, Faculty of Computer Science, Electronics and Telecommunications, Kraków, Poland*
- ^p *LIFAELS, La Salle, Universitat Ramon Llull, Barcelona, Spain*
- ^q *Hanoi University of Science, Hanoi, Viet Nam*
- ^r *Università di Padova, Padova, Italy*
- ^s *Università di Pisa, Pisa, Italy*
- ^t *Scuola Normale Superiore, Pisa, Italy*
- ^u *Università degli Studi di Milano, Milano, Italy*

1 Introduction

Measurements in proton-nucleus collisions can serve as references for nucleus-nucleus collisions and be used as inputs for the determination of nuclear parton distribution functions (nPDF) [1]. The nPDF, $f_a^{i,A}(x_A, Q^2)$, is defined as a function of the momentum fraction, x_A , of a certain parton type a inside the nucleon i bound in a nucleus A for an energy scale Q^2 . It is usually parametrised by the nuclear modification factor, $R_a^A(x_A, Q^2)$, which represents the ratio between the nPDF and the corresponding free nucleon baseline PDF, $f_a^i(x, Q^2)$. For x_A less than 0.02, R_a^A is smaller than unity as the coherence length of the interaction is larger than the nucleon-nucleon distance inside the nucleus (shadowing effect) [2]. For x_A -values between about 0.4 and 0.8, R_a^A is less than unity due to the EMC effect [3]. For values of x_A close to 1.0, R_a^A is predicted to be greater than unity due to Fermi motion [4]. In the intermediate region between the regimes of shadowing and the EMC effect, R_a^A is also predicted to be greater than unity because of the sum rule of PDFs (anti-shadowing) [5–7].

The most recent available nPDF sets [8–11] are primarily based on data from fixed target experiments (deep inelastic scattering (DIS) and Drell-Yan processes) and, in particular cases, on additional data from d-Au collisions at RHIC and from neutrino DIS. As a consequence of the kinematic range in these experiments, nPDFs for Q^2 larger than 10 GeV² have either no or only weak direct constraints for values of x_A smaller than 0.01 and x_A close to one [1, 4].

Since measurements of electroweak boson production in the forward direction of proton-lead collisions involve small x_A -values and in the backward direction x_A -values close to one, they can serve as input to nPDF fits with a significant constraining power, especially at small x_A -values. ‘Forward’ refers to positive rapidity values defined relative to the direction of the proton beam, ‘backward’ to negative rapidity values. No measurement of electroweak boson production in proton-lead collisions has yet been performed, while their production in lead-lead collisions has been measured for central rapidities [12, 13].

Due to its rapidity coverage, the LHCb experiment has the ability to probe x_A down to very small, but also up to very large values. The sensitivity of x_A at a centre-of-mass energy per proton-nucleon pair of $\sqrt{s_{NN}} = 5$ TeV varies from 2×10^{-4} to 3×10^{-3} in the forward case and from 0.2 to 1.0 in the backward case at an energy scale $Q^2 = M_Z^2$.

In this paper a first measurement of the Z production cross-section in proton-lead collisions in the forward and backward region is presented. The measurement uses Z bosons reconstructed in the $\mu^+\mu^-$ final state and is performed in a similar manner to the Z production measurements in pp collisions described in Refs. [14] and [15]. The fiducial region in the laboratory frame is defined by: the transverse momenta, p_T , of the muons, which must be larger than 20 GeV/ c ; their pseudorapidities, η , required to be between 2.0 and 4.5; and the invariant dimuon mass, which is restricted to be between 60 and 120 GeV/ c^2 . The cross-section is measured as

$$\sigma_{Z \rightarrow \mu^+\mu^-} = \frac{N_{\text{cand}} \times \rho}{\mathcal{L} \times \varepsilon}, \quad (1)$$

where N_{cand} is the number of selected Z candidates, ρ the purity of the sample, \mathcal{L} the integrated luminosity and ε the total efficiency.

The results are compared to predictions at next-to-next-to-leading order (NNLO [16]) in perturbative quantum chromodynamics with and without nuclear effects [8].

2 Detector and software

The LHCb detector [17] is a single-arm forward spectrometer covering the pseudorapidity range $2 < \eta < 5$, designed for the study of particles containing b or c quarks. The detector includes a high-precision tracking system consisting of a silicon-strip vertex detector surrounding the interaction region, a large-area silicon-strip detector located upstream of a dipole magnet with a bending power of about 4 Tm, and three stations of silicon-strip detectors and straw drift tubes [18] placed downstream. The combined tracking system provides a momentum measurement with relative uncertainty that varies from 0.4% at 5 GeV/ c to 0.6% at 100 GeV/ c , and an impact parameter resolution of 20 μm for tracks with large transverse momentum. The energy of photons, electrons and hadrons is measured by a calorimeter system consisting of scintillating-pad and preshower detectors, an electromagnetic calorimeter (ECAL) and a hadronic calorimeter (HCAL). Muons are identified by a system composed of alternating layers of iron and multiwire proportional chambers [19]. The trigger [20] consists of a hardware stage, based on information from the calorimeter and muon systems, followed by a software stage, which applies a full event reconstruction.

During data taking of proton-lead collisions, the hardware stage of the trigger accepted all non-empty bunch crossings, and the software stage accepted events with at least one well-reconstructed track matched to hits in the muon system with a momentum above 8 GeV/ c and p_{T} above 4.8 GeV/ c . In order to avoid events with high hit multiplicity, which dominate the processing time in the software trigger, global event cuts (GEC) are applied on hit multiplicities in the tracking detectors.

Simulated pp collisions used in the estimation of the purity are generated using PYTHIA6 [21] with a specific LHCb configuration [22]. Decays of hadronic particles are described by EVTGEN [23], in which final state radiation is generated using PHOTOS [24]. The interaction of the generated particles with the detector and its response are implemented using the GEANT4 toolkit [25] as described in Ref. [26].

To study the kinematics in proton-lead collisions, dedicated samples of simulated events at parton level are generated with PYTHIA8 [27] together with the MSTW08 PDF set [28]. These samples contain $Z \rightarrow \mu^+ \mu^-$ decays produced in proton-proton and proton-neutron collisions at a centre-of-mass energy of $\sqrt{s} = 5 \text{ TeV}$ with beam energies corresponding to the energy of the proton beam and the energy per nucleon in the lead beam, respectively.

3 Data samples and candidate selection

The analysis is based on data samples of proton-lead collisions that correspond to integrated luminosities of $1.099 \pm 0.021 \text{ nb}^{-1}$ in the forward and $0.521 \pm 0.011 \text{ nb}^{-1}$ in the backward direction. The integrated luminosity has been calibrated by Van der Meer scans separately for each beam configuration [29,30]. The energy of the proton beam is $E_p = 3988 \pm 26 \text{ GeV}$ while the energy of the lead beam per nucleon is $E_N = 1572 \pm 10 \text{ GeV}$. This gives a centre-of-mass energy per proton-nucleon pair of $\sqrt{s_{NN}} = 5008 \pm 33 \text{ GeV}$, which is approximated to 5 TeV [31]. Due to the asymmetric beam energy there is a rapidity shift between the rapidity y_{Lab} in the laboratory and y in the centre-of-mass frame of $\Delta y = y_{\text{lab}} - y = +0.47$.

The Z candidates are selected from reconstructed pairs of oppositely charged particles that are identified as muons by matched hits in the muon system and that are inside the considered fiducial region. Selection criteria are applied to reject background candidates that fake $Z \rightarrow \mu^+\mu^-$ decays: the impact parameter of each track with respect to the closest primary vertex must be less than $100 \mu\text{m}$, and the sum of the energies measured in the ECAL and HCAL associated to each track has to be less than 0.5 times the track momentum measured in the tracking system. The χ^2 -probability of the track fit is required to be larger than 1% for both tracks.

Figure 1 shows the invariant mass distribution of the selected candidates for the two beam configurations together with the predictions from simulation. There is a good agreement between data and simulation. In total, eleven candidates are selected in the forward sample and four in the backward sample. The rapidity distributions of the Z candidates are shown in Fig. 2.

The efficiencies and the purity are studied with a sample of Z candidates from pp collisions at $\sqrt{s} = 8 \text{ TeV}$ corresponding to 2 fb^{-1} of integrated luminosity. These Z

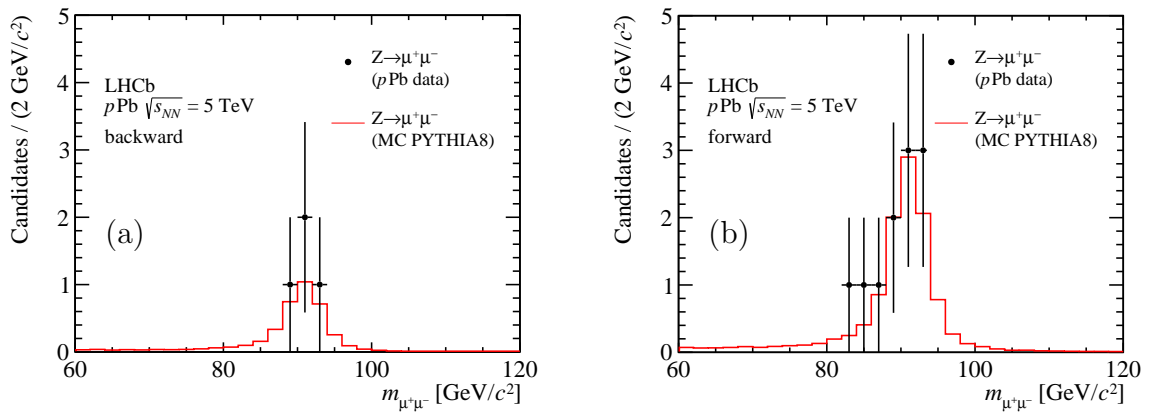


Figure 1: Invariant dimuon mass distribution of selected Z candidates in (a) the backward and (b) the forward sample are shown by the black data points with error bars. The red line shows the distribution obtained from simulation using PYTHIA8 with the MSTW08 PDF set normalised to the number of observed candidates.

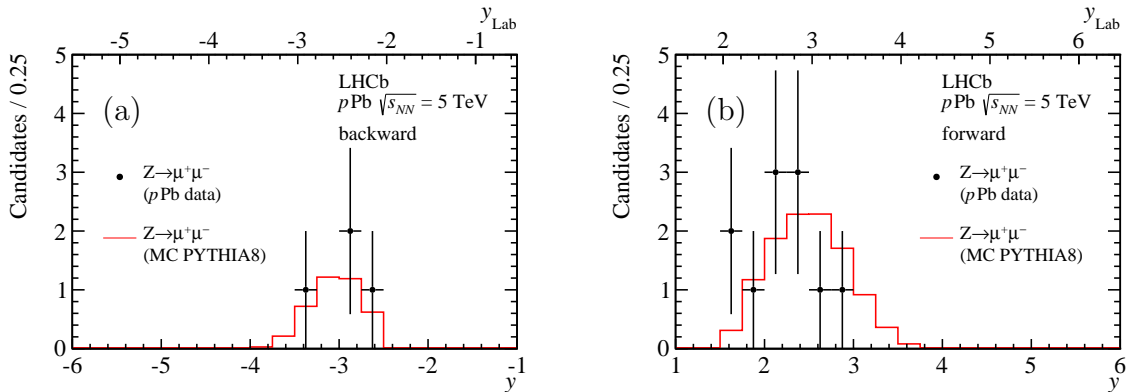


Figure 2: Rapidity distribution of selected Z candidates in (a) the backward and in (b) the forward sample are shown by the black data points. The red line shows the distribution obtained from simulation using PYTHIA8 with the MSTW08 PDF set normalised to the number of observed candidates. The top x -axis shows the rapidity, y_{Lab} , in the laboratory frame, the bottom one the rapidity, y , in the centre-of-mass frame.

candidates have to fulfil the same selection criteria as those in proton-lead collisions. Since the purity and efficiencies depend on the multiplicity, the difference in track multiplicity is taken into account by reweighting the candidates from the pp sample to match the multiplicity in proton-lead collisions. The reweighting is performed using the observed ratio of the track multiplicity distributions of events containing J/ψ candidates in proton-lead and proton-proton collisions.

4 Purity and efficiency determination

The purity estimation considers two background sources. The first comprises candidates where at least one of the muons is a misidentified hadron. This background source is expected to have the same absolute abundance in oppositely charged as identically charged dimuon combinations and the relative fraction is estimated from the number of candidates observed in a sample of same-sign candidates and amounts to about 0.16%.

The second source, referred to as heavy-quark background, originates from semileptonic decays of $b\bar{b}$ and $c\bar{c}$ pairs into oppositely charged muon pairs. Two background-enriched samples are used. In the first sample, the vertex fit χ^2 per degree of freedom of the dimuon vertex is required to be larger than 70 to reject signal combinations. In the second sample, an anti-isolation criterion on each muon rejects signal combinations: the p_{T} of the muon has to be less than 70% of the summed p_{T} of the tracks that differ in η and the azimuthal angle, ϕ , with respect to the muon track by less than $\sqrt{\Delta\eta^2 + \Delta\phi^2} = 0.5$. In both cases, the efficiency of the cuts for the heavy-quark background is estimated from simulation. The relative background contribution is estimated from the efficiency-corrected

background yield in the signal mass window. The two samples yield consistent results of about 0.20 %.

The weighted average of the two estimates for heavy-quark background is added to the contribution from misidentified hadrons, which gives a purity, ρ , of $(99.74 \pm 0.06)\%$ for the forward and $(99.63 \pm 0.05)\%$ for the backward direction.

The total efficiency ε factorises into two parts as $\varepsilon = \varepsilon^{\text{GEC}} \times \varepsilon^{\text{cand}}$. The first term, ε^{GEC} , is related to the GEC, based on the occupancy in the vertex and tracking detectors. The second term, $\varepsilon^{\text{cand}}$, accounts for the reconstruction, selection, trigger and muon-identification efficiency of the $Z \rightarrow \mu^+ \mu^-$ decays.

The value of ε^{GEC} is estimated from the occupancy distributions in events with J/ψ candidates from proton-lead collisions following the method described in Ref. [32]. While the GEC do not remove events in the forward beam configuration, they retain $(97.8 \pm 1.9)\%$ in the backward configuration.

The reconstruction, selection, trigger and muon-identification efficiencies are estimated by tag-and-probe methods as described in Ref. [14]. The tag-and-probe methods use track-multiplicity-reweighted Z candidates from pp collisions at $\sqrt{s} = 8$ TeV. These efficiencies are determined as functions of the muon pseudorapidity. As the sample size of the Z candidates in proton-lead collisions is very small, the overall value of $\varepsilon^{\text{cand}}$ is evaluated by folding the efficiency as a function of the pseudorapidity with the η distribution of muons. These distributions are obtained from simulated Z bosons produced in pp and pn collisions to mimic proton-lead collisions. The value of $\varepsilon^{\text{cand}}$ is $(74.1 \pm 6.2)\%$ for the forward and $(72.8 \pm 6.3)\%$ for the backward direction.

5 Systematic uncertainties

Five potential sources of systematic uncertainties are considered:

1. The uncertainty on the sample purity is due to the statistical uncertainty on the data samples used in its determination. It also includes the statistical uncertainty on the efficiency determination of the cuts to obtain the samples enriched by the heavy-quark background using simulation. A further contribution is included for potential differences in the centre-of-mass energy dependence of the signal and background processes.
2. The uncertainty on the GEC efficiency is estimated by changing the functional form used to describe the occupancy distributions. Possible differences in the occupancy distributions between events containing J/ψ and those containing Z candidates using data from pp collisions at $\sqrt{s} = 8$ TeV are taken into account.
3. The uncertainty on the candidate efficiency includes the uncertainties on the reconstruction, selection, trigger and muon-identification efficiencies. It is based on the statistical uncertainty of the measured efficiencies as well as on the uncertainty of the muon pseudorapidity spectrum from simulation used to obtain the average efficiency values.

Table 1: Systematic uncertainties in the cross-section calculation for $\sigma_{Z\rightarrow\mu^+\mu^-}$. The uncertainties on ρ and $\varepsilon^{\text{cand}}$ are assumed to be fully correlated between the forward and the backward sample.

Source	Forward	Backward
Sample purity	0.5 %	0.5 %
GEC efficiency	0.0 %	1.9 %
Candidate efficiency	8.4 %	8.7 %
Multiplicity reweighting	1.5 %	2.0 %
Luminosity	1.9 %	2.1 %
Total	8.8 %	9.4 %

- The uncertainty on the track multiplicity reweighting is assigned as the relative difference in the ratio $\rho/\varepsilon^{\text{cand}}$ with and without applying the reweighting in the determination of the purity as well as the reconstruction, selection, trigger and muon-identification efficiencies.
- The uncertainty on the luminosity is based on the statistical and systematic uncertainties of the calibration method mentioned in Sect. 3.

All systematic uncertainties are listed in Table 1 and are added in quadrature to give the total systematic uncertainty as they are considered uncorrelated.

6 Results

The Z production cross-sections in proton-lead collisions measured in the fiducial region of $60 < m_{\mu^+\mu^-} < 120 \text{ GeV}/c^2$, $p_{\text{T}}(\mu^\pm) > 20 \text{ GeV}/c$ and $2.0 < \eta(\mu^\pm) < 4.5$ are

$$\sigma_{Z\rightarrow\mu^+\mu^-}(\text{fwd}) = 13.5_{-4.0}^{+5.4}(\text{stat.}) \pm 1.2(\text{syst.}) \text{ nb}$$

in the forward direction, and

$$\sigma_{Z\rightarrow\mu^+\mu^-}(\text{bwd}) = 10.7_{-5.1}^{+8.4}(\text{stat.}) \pm 1.0(\text{syst.}) \text{ nb}$$

in the backward direction. The first uncertainty is statistical, defined as the 68 % confidence interval with symmetric coverage assuming that the number of candidates follows a Poisson distribution, and the second uncertainty is systematic.

The cross-sections calculated at NNLO using FEWZ [16] and the MSTW08 PDF set [28] are listed in Table 2. The nuclear modifications to the cross-sections are parametrised by the EPS09 nPDF set at next-to-leading order (NLO) [8]. The obtained values are in agreement with the results of the measurements. The measurement is not precise enough

to make any conclusion about the presence of nuclear effects. Figure 3 shows a comparison of the experimental results and the theoretical predictions.

The statistical significance of the Z signal is evaluated by the probability that a Poisson distribution with the expected background yield $N_{\text{bkg}}^{\text{th}} = \sigma_{Z \rightarrow \mu^+ \mu^-}^{\text{th}} \varepsilon^{\text{GEC}} \varepsilon^{\text{cand}} \mathcal{L}(1 - \rho)/\rho$ as expectation value fluctuates to the observed signal. The theoretical cross-section $\sigma_{Z \rightarrow \mu^+ \mu^-}^{\text{th}}$ is defined as the value obtained from NNLO calculation using FEWZ and nuclear modifications based on the EPS09 nPDF set. This gives a significance of 10.4σ for the Z signal in the forward direction and 6.8σ for the backward direction.

As shown by the calculations using nPDF sets, but also from theoretical calculations [33] using the leading-twist approach to model the effect of shadowing and anti-shadowing [7], a suppression of the cross-section in the forward direction is expected while for the backward direction only a small effect is predicted.

A particularly sensitive variable to detect nuclear modifications is the forward-backward ratio, R_{FB} , defined as

$$R_{\text{FB}}(\sqrt{s_{NN}}, |y|) \equiv \frac{\sigma(\sqrt{s_{NN}}, +|y|)}{\sigma(\sqrt{s_{NN}}, -|y|)}. \quad (2)$$

In LHCb, R_{FB} can be measured in the overlap region $2.5 < |y| < 4.0$ of the Z rapidity in the centre-of-mass frame of the two beam configurations. The cross-section ratio determined for this range including acceptance corrections should be one without any nuclear effects. The predicted value from NNLO calculation using FEWZ with the MSTW08 PDF set and the nuclear modifications of the PDF from the EPS09 set at NLO is $R_{\text{FB}}(2.5 < |y| < 4.0) = 0.943_{-0.027}^{+0.012}$; the quoted uncertainty is due to the uncertainties on the nPDF. The scale and PDF uncertainties cancel in the ratio.

The value of R_{FB} measured in the overlap region $2.5 < |y| < 4.0$ is defined as

$$R_{\text{FB}}(2.5 < |y| < 4.0) = \frac{N_{\text{cand,fwd}}}{N_{\text{cand,bwd}}} \times \frac{\rho_{\text{fwd}}}{\rho_{\text{bwd}}} \times \frac{\varepsilon_{\text{bwd}}}{\varepsilon_{\text{fwd}}} \times \frac{\mathcal{L}_{\text{bwd}}}{\mathcal{L}_{\text{fwd}}} \times \frac{1}{\beta}, \quad (3)$$

where β is the correction factor for the difference in the detector acceptance of the muons between the forward and backward directions. It is evaluated using NNLO FEWZ calcula-

Table 2: $Z \rightarrow \mu^+ \mu^-$ cross-section predictions based on NNLO calculations using FEWZ with the MSTW08 PDF set. The nuclear modifications are parametrised by the EPS09 nPDF set. The first uncertainty is the scale uncertainty evaluated by changing the renormalisation and factorisation scales by a factor two up and down. The second one comes from the uncertainties on the PDF and the third in case of the predictions with nuclear effects from the nPDF.

Theory setup	$\sigma_{Z \rightarrow \mu^+ \mu^-}$ [nb]	
	Forward	Backward
No nuclear effects	$14.48_{-0.09-0.27}^{+0.12+0.30}$	$2.81_{-0.03-0.06}^{+0.03+0.07}$
With nuclear effects (EPS09)	$13.12_{-0.08-0.24-0.10}^{+0.11+0.27+0.03}$	$2.61_{-0.03-0.06-0.08}^{+0.03+0.07+0.03}$

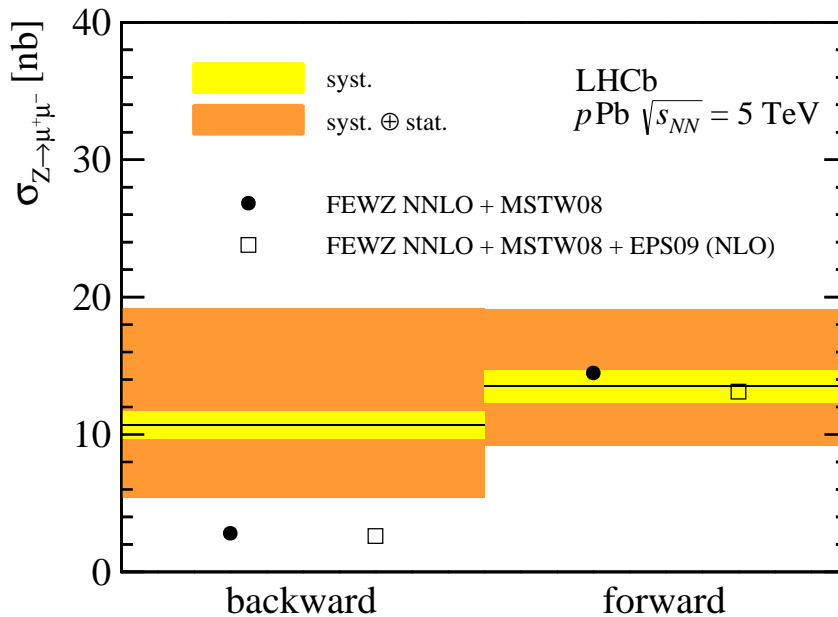


Figure 3: Experimental results and the theoretical predictions for the $Z \rightarrow \mu^+ \mu^-$ production cross-section. The inner error bars of the experimental results show the systematic uncertainties. The uncertainties on the theoretical predictions are negligible compared to those on the experimental results.

tions to be $\beta = 2.419_{-0.000}^{+0.127}(\text{theo.}) \pm 0.008(\text{num.})_{-0.010}^{+0.009}(\text{PDF})$, where the first uncertainty is from the variation of the renormalisation and factorisation scale, the second the numerical and the last the uncertainty from the PDF uncertainties. The scale variation always leads to an enhancement of β .

The numbers of candidates in the common y range are 2 in the forward and 4 in the backward samples. The measured value for R_{FB} is

$$R_{\text{FB}}(2.5 < |y| < 4.0) = 0.094_{-0.062}^{+0.104}(\text{stat.})_{-0.007}^{+0.004}(\text{syst.}),$$

where the first uncertainty is statistical, defined as the 68% confidence interval with symmetric coverage. The 99.7% (*i.e.* 3σ) confidence interval with symmetric coverage is $[0.002, 1.626]$ whereas the asymmetry of the interval around the central value is due to non-Gaussian statistical uncertainties. The second uncertainty is systematic and includes also the uncertainty on the acceptance correction factor β . The systematic uncertainties between the forward and the backward directions on the purity and the reconstruction, selection, trigger and muon-identification efficiency are assumed to be fully correlated. The probability to observe a value of R_{FB} no larger than that measured, assuming no nuclear modifications (*i.e.* the true value is $R_{\text{FB}} = 1$), is 1.2%. This corresponds to a deviation with a 2.2σ significance. The probability is estimated with a toy Monte Carlo assuming

Poissonian distributions for the number of candidates.

7 Conclusions

Measurements of Z production in proton-lead collisions at LHCb at $\sqrt{s_{NN}} = 5$ TeV in the forward and backward directions, with data corresponding to 1.1 and 0.5 nb⁻¹ of integrated luminosity, respectively, have been performed.

The cross-section is measured to be

$$\sigma_{Z \rightarrow \mu^+ \mu^-}(\text{fwd}) = 13.5_{-4.0}^{+5.4}(\text{stat.}) \pm 1.2(\text{syst.}) \text{ nb},$$

in the forward direction, and

$$\sigma_{Z \rightarrow \mu^+ \mu^-}(\text{bwd}) = 10.7_{-5.1}^{+8.4}(\text{stat.}) \pm 1.0(\text{syst.}) \text{ nb}$$

in the backward direction. These values are in agreement with predictions, although the production of Z bosons in the backward direction appears to be higher than predictions. The fiducial region is defined by $2.0 < \eta(\mu^\pm) < 4.5$, $p_T(\mu^\pm) > 20$ GeV/ c and $60 < m_{\mu^+ \mu^-} < 120$ GeV/ c^2 . The forward-backward ratio R_{FB} in the Z rapidity interval $2.5 < |y| < 4.0$ in the centre-of-mass frame is found to be lower than expectations, and corresponds to a 2.2σ deviation from $R_{\text{FB}} = 1$.

The statistical precision of the measured cross-sections prevents conclusions on the presence of nuclear effects. The first observation of Z production in proton-nucleus collisions demonstrates the excellent potential of the study of electroweak bosons in proton-lead collisions at LHCb.

Acknowledgements

We express our gratitude to our colleagues in the CERN accelerator departments for the excellent performance of the LHC. We thank the technical and administrative staff at the LHCb institutes. We acknowledge support from CERN and from the national agencies: CAPES, CNPq, FAPERJ and FINEP (Brazil); NSFC (China); CNRS/IN2P3 (France); BMBF, DFG, HGF and MPG (Germany); SFI (Ireland); INFN (Italy); FOM and NWO (The Netherlands); MNiSW and NCN (Poland); MEN/IFA (Romania); MinES and FANO (Russia); MinECo (Spain); SNSF and SER (Switzerland); NASU (Ukraine); STFC (United Kingdom); NSF (USA). The Tier1 computing centres are supported by IN2P3 (France), KIT and BMBF (Germany), INFN (Italy), NWO and SURF (The Netherlands), PIC (Spain), GridPP (United Kingdom). We are indebted to the communities behind the multiple open source software packages on which we depend. We are also thankful for the computing resources and the access to software R&D tools provided by Yandex LLC (Russia). Individual groups or members have received support from EPLANET, Marie Skłodowska-Curie Actions and ERC (European Union), Conseil général de Haute-Savoie,

Labex ENIGMASS and OCEVU, Région Auvergne (France), RFBR (Russia), XuntaGal and GENCAT (Spain), Royal Society and Royal Commission for the Exhibition of 1851 (United Kingdom).

References

- [1] C. Salgado *et al.*, *Proton-nucleus collisions at the LHC: scientific opportunities and requirements*, J. Phys. **G39** (2012) 015010, [arXiv:1105.3919](#).
- [2] R. Glauber, *Cross-sections in deuterium at high-energies*, Phys. Rev. **100** (1955) 242.
- [3] European Muon collaboration (EMC), J. Aubert *et al.*, *The ratio of the nucleon structure functions F_2^N for iron and deuterium*, Phys. Lett. **B123** (1983) 275.
- [4] K. J. Eskola, *Global analysis of nuclear PDFs - latest developments*, Nucl. Phys. **A 910-911** (2013) 163, [arXiv:1209.1546](#); H. Paukkunen, *Nuclear PDFs in the beginning of the LHC era*, [arXiv:1401.2345](#).
- [5] R. Glauber, *Deuteron stripping processes at high energies*, Phys. Rev. **99** (1955) 1515.
- [6] D. Kharzeev and H. Satz, *The quantum-mechanical origin of nuclear shadowing*, Phys. Lett. **B327** (1994) 361.
- [7] L. Frankfurt, V. Guzey, and M. Strikman, *Leading twist nuclear shadowing phenomena in hard processes with nuclei*, Phys. Rept. **512** (2012) 255, [arXiv:1106.2091](#).
- [8] K. Eskola, H. Paukkunen, and C. Salgado, *EPS09: A new generation of NLO and LO nuclear parton distribution Functions*, JHEP **04** (2009) 065, [arXiv:0902.4154](#).
- [9] M. Hirai, S. Kumano, and T.-H. Nagai, *Determination of nuclear parton distribution functions and their uncertainties in next-to-leading order*, Phys. Rev. **C76** (2007) 065207, [arXiv:0709.3038](#); M. Hirai, S. Kumano, and T.-H. Nagai, *Global NLO analysis of nuclear parton distribution functions*, AIP Conf. Proc. **981** (2008) 265, [arXiv:0711.2557](#).
- [10] D. de Florian, R. Sassot, P. Zurita, and M. Stratmann, *Global analysis of nuclear parton distributions*, Phys. Rev. **D85** (2012) 074028, [arXiv:1112.6324](#).
- [11] I. Schienbein *et al.*, *PDF nuclear corrections for charged and neutral current processes*, Phys. Rev. **D80** (2009) 094004, [arXiv:0907.2357](#); K. Kovarik *et al.*, *Nuclear corrections in neutrino-nucleus DIS and their compatibility with global NPDF analyses*, Phys. Rev. Lett. **106** (2011) 122301, [arXiv:1012.0286](#); K. Kovarik *et al.*, *CTEQ nuclear parton distribution functions*, PoS **DIS2013** (2013) 274, [arXiv:1307.3454](#).
- [12] ATLAS collaboration, G. Aad *et al.*, *Measurement of the centrality dependence of J/ψ yields and observation of Z production in lead-lead collisions with the ATLAS detector at the LHC*, Phys. Lett. **B697** (2011) 294, [arXiv:1012.5419](#); ATLAS collaboration, *Measurements of W Boson Yields in $Pb+Pb$ at 2.76 TeV/nucleon via single muons with the ATLAS detector*, ATLAS-CONF-2011-078.

- [13] CMS collaboration, S. Chatrchyan *et al.*, *Study of Z boson production in PbPb collisions at nucleon-nucleon centre of mass energy = 2.76 TeV*, Phys. Rev. Lett. **106** (2011) 212301, [arXiv:1102.5435](#); CMS collaboration, S. Chatrchyan *et al.*, *Study of W boson production in PbPb and pp collisions at $\sqrt{s_{NN}} = 2.76$ TeV*, Phys. Lett. **B715** (2012) 66, [arXiv:1205.6334](#).
- [14] LHCb collaboration, R. Aaij *et al.*, *Inclusive W and Z production in the forward region at $\sqrt{s} = 7$ TeV*, JHEP **06** (2012) 058, [arXiv:1204.1620](#).
- [15] LHCb collaboration, *Measurement of the cross section for $Z \rightarrow \mu^+\mu^-$ production with 1.0 fb^{-1} of pp collisions at $\sqrt{s} = 7$ TeV*, LHCb-CONF-2013-007.
- [16] R. Gavin, Y. Li, F. Petriello, and S. Quackenbush, *FEWZ 2.0: A code for hadronic Z production at next-to-next-to-leading order*, Comput. Phys. Commun. **182** (2011) 2388, [arXiv:1011.3540](#); Y. Li and F. Petriello, *Combining QCD and electroweak corrections to dilepton production in the framework of the FEWZ simulation code*, Phys. Rev. **D86** (2012) 094034, [arXiv:1208.5967](#).
- [17] LHCb collaboration, A. A. Alves Jr. *et al.*, *The LHCb detector at the LHC*, JINST **3** (2008) S08005.
- [18] R. Arink *et al.*, *Performance of the LHCb outer tracker*, JINST **9** (2014) P01002, [arXiv:1311.3893](#).
- [19] A. A. Alves Jr. *et al.*, *Performance of the LHCb muon system*, JINST **8** (2013) P02022, [arXiv:1211.1346](#).
- [20] R. Aaij *et al.*, *The LHCb trigger and its performance in 2011*, JINST **8** (2013) P04022, [arXiv:1211.3055](#).
- [21] T. Sjöstrand, S. Mrenna, and P. Skands, *PYTHIA 6.4 physics and manual*, JHEP **05** (2006) 026, [arXiv:hep-ph/0603175](#).
- [22] I. Belyaev *et al.*, *Handling of the generation of primary events in GAUSS, the LHCb simulation framework*, Nuclear Science Symposium Conference Record (NSS/MIC) **IEEE** (2010) 1155.
- [23] D. J. Lange, *The EVTGEN particle decay simulation package*, Nucl. Instrum. Meth. **A462** (2001) 152.
- [24] P. Golonka and Z. Was, *PHOTOS Monte Carlo: a precision tool for QED corrections in Z and W decays*, Eur. Phys. J. **C45** (2006) 97, [arXiv:hep-ph/0506026](#).
- [25] Geant4 collaboration, J. Allison *et al.*, *GEANT4 developments and applications*, IEEE Trans. Nucl. Sci. **53** (2006) 270; Geant4 collaboration, S. Agostinelli *et al.*, *GEANT4: a simulation toolkit*, Nucl. Instrum. Meth. **A506** (2003) 250.

- [26] M. Clemencic *et al.*, *The LHCb simulation application, GAUSS: design, evolution and experience*, J. Phys. Conf. Ser. **331** (2011) 032023.
- [27] T. Sjöstrand, S. Mrenna, and P. Skands, *A brief introduction to PYTHIA 8.1*, Comput. Phys. Commun. **178** (2008) 852, [arXiv:0710.3820](#).
- [28] A. Martin, W. Stirling, R. Thorne, and G. Watt, *Parton distributions for the LHC*, Eur. Phys. J. **C63** (2009) 189, [arXiv:0901.0002](#).
- [29] S. van der Meer, *Calibration of the effective beam height in the ISR*, CERN-ISR-PO-68-31, 1968.
- [30] H. Burkhardt and P. Grafstrom, *Absolute luminosity from machine parameters*, CERN-LHC-PROJECT-REPORT-1019, 2007.
- [31] J. Wenninger, *Energy calibration of the LHC beams at 4 TeV*, CERN-ATS-2013-040, Geneva, May, 2013.
- [32] LHCb collaboration, R. Aaij *et al.*, *Study of J/ψ production and cold nuclear matter effects in pPb collisions at $\sqrt{s_{NN}} = 5$ TeV*, JHEP **02** (2014) 072, [arXiv:1308.6729](#).
- [33] V. Guzey *et al.*, *Massive neutral gauge boson production as a probe of nuclear modifications of parton distributions at the LHC*, Eur. Phys. J. **A49** (2013) 35, [arXiv:1212.5344](#).